Molecular Dynamics Study on the Mechanism of Graphene Oxide to Destabilize Oil-Water Emulsion

Tu Lan,[†,‡] Hongbo Zeng,[*,†] and Tian Tang,[*,‡]

[†]*Department of Chemical and Materials Engineering and* [‡]*Department of Mechanical Engineering, University of Alberta, Edmonton, Alberta T6G 1H9, Canada*

**Corresponding authors:*

Phone: +1-780-492-1044. E-mail: hongbo.zeng@ualberta.ca (H.Z.).

Phone: +1-780-492-5467. E-mail: tian.tang@ualberta.ca (T.T.).

ABSTRACT

Previous experiments have demonstrated the capability of graphene oxide (GO) to destabilize oil-in-water (O/W) and water-in-oil (W/O) emulsions, although there are debates on the underlying mechanism. Using molecular dynamics simulations, this work targets an atomistic level understanding of the mechanism for GO to destabilize O/W and W/O emulsions in the presence of violanthrone-79 (VO-79), a model compound for asphaltene. For both types of emulsions, a GO/VO-79 binary film is formed on the oil/water interface, which can stabilize VO-79 on the interface. Detailed structural analysis shows that the majority of GO in the binary film are parallel to the interface and cause VO-79 to align with them, changing the original interface morphology. The results favor the mechanism that GO destabilizes W/O or O/W emulsions by first forming a film around the emulsion droplets and then enhancing the adhesion between droplets, or between a droplet and the macroscopic oil/water interface, through film-film interactions. Additional interfacial tension (IFT) calculations confirm that GO can increase the toluene/water IFT in the presence of VO-79, which is beneficial for emulsion destabilization.

1. INTRODUCTION

Graphene oxide (GO), a material typically prepared by reacting graphite powder with strong oxidizing agents in concentrated sulfuric acid,[1] contains oxygenated functional groups on its basal plane and edges.[2,3] It is a two-dimensional material that exhibits amphiphilic property: hydrophilic on the periphery while mostly hydrophobic at the center.[4] Although GO has been discovered for more than a century, in the past decade there has been an increasing interest in exploring its new applications, for example as a "surfactant",[5-9] fillers in composites,[10-13] and in liquid crystal devices.[14-17]

Due to its amphiphilic property and unique interfacial behavior,[5] GO has been recently explored as a potential demulsifier for emulsions.[18-23] Liu *et al*. studied the demulsification performance of GO for crude oil-in-water (O/W) emulsions.[18] These emulsions can be very stable due to the presence of a protective film on the oil/water interface formed by asphaltenes.[24,25] Upon the addition of GO and proper mixing, it was observed that oil separated from water within a few minutes. The effect of pH on the demulsification efficiency indicated that GO was effective under acidic or neutral conditions, but not in alkaline solution.[18] The same group further investigated the destabilization of O/W emulsions by variations of GO, such as reduced graphene oxide (rGO) and magnetic graphene oxide (M-GO).[19,20] It was found that the demulsification performance of rGO could be considerably improved by increasing the reduction degree,[19] and M-GO can be recycled 6–7 times without losing its demulsification capability.[20] Such multi-recycling capability was also observed in the work of Ma *et al.*[21] where they synthesized a bifunctional demulsifier, octadecyltrimethoxysilane (ODTS) modified magnetite/reduced graphene oxide (MRGO@ODTS). It can effectively demulsify both O/W and W/O emulsions and there is no decline in its demulsification efficiency within 10 cycles. Fang *et al*. investigated the demulsification performance of GO for O/W emulsions in oily wastewater.[23] It was seen that the stability of the emulsion was destroyed immediately upon the addition of GO, leading to fast oil-water separation.

Different mechanisms were proposed for the demulsification using GO. For the O/W emulsion, Liu *et al*. proposed that GO interacted strongly with asphaltenes on the oil/water interface and was able to pull asphaltenes away from the interface.[18-20] Such interactions led to partial destruction of the asphaltenes film and subsequently coalescence of the oil droplets, facilitating the oil-water separation. Fang *et al*., on the other hand, proposed another demulsification mechanism[23] based on experiments of GO

assembly at oil/water interface in the presence of surfactants, e.g., cetyltrimethylammonium bromide (CTAB) and sodium dodecyl sulfate (SDS).[22] It was found that the attractive interaction between CTAB and GO facilitated the assembly of GO at the oil/water interface and the emulsions became more unstable. In contrast, the electrostatic repulsion between SDS and GO restricted the assembly of GO at the interface and led to persistent stability of the emulsions. Considering these findings, it was hypothesized that a GO could adhere to the asphaltenes and assemble into a new GO film wrapping the oil droplets. When an oil droplet moves close to the macroscopic oil/water interface, the GO film around the droplet could interact with the GO assembled at the macroscopic interface, draining the oil drop into the bulk oil phase. In other words, the separation of oil from water was enabled by the interaction between assembled GO films.

The two hypotheses above are both interesting, but direct verification using experiments is not possible due to the limitation in resolution. With the assistance of molecular dynamics (MD) simulations, Liu *et al*. studied the destabilization of W/O emulsion by ethyl cellulose (EC). EC molecules were found to gradually pull away asphaltenes pre-adsorbed on a toluene/water interface, which could then imply partial destruction of asphaltenes film and the coalescence of water droplets from a W/O emulsion.[26] For GO as a demulsifier, although Fang *et al*. attempted to generate some insights from MD simulations, their simulations were very simplistic.[23] Only 4 GO nanosheets were simulated at an oil/water interface, in absence of asphaltenes and for a very short simulation time of 1 ns. Therefore, direct evidence for the demulsification mechanism of GO is still lacking. Motivated by this, we performed a series of MD simulations to systematically investigate the behaviors of GO at the oil/water interface in the presence of a model asphaltene compound. Through the simulations, we address the likelihood of GO pulling asphaltenes from the interface to the bulk and that of GO forming an additional film at the interface. By properly designing the simulations, we can mimic the situations of both O/W and W/O emulsions, and study whether GO may play different roles depending on the type of emulsion. This work improves the fundamental understanding on the demulsification mechanism of GO from a molecular perspective.

2. METHODS

2.1 Models and Systems Simulated

Each system simulated in this work contains an oil/water interface in the presence of model asphaltenes. The oil phase was represented by toluene, considering its natural occurrence in crude oil. Violanthrone-79 (VO-79, $C_{50}H_{48}O_4$) was chosen as the model for asphaltene. VO-79 has one central polyaromatic core (PAC) and two side chains, resembling the island-type structure of asphaltene proposed in the literature,[27] and has been employed widely to study the behavior of asphaltenes at oil/water interface.[28-32] The model for GO ($C_{106}H_{26}O_{20}$) was based on experimental characterizations and simulations in previous studies.[33,34] All the carboxyl and hydroxyl groups have net zero charge to mimick an acidic environment where GO has been shown to be effective in demulsification.[18] Molecular structures of VO-79 and GO are shown in Figure 1.

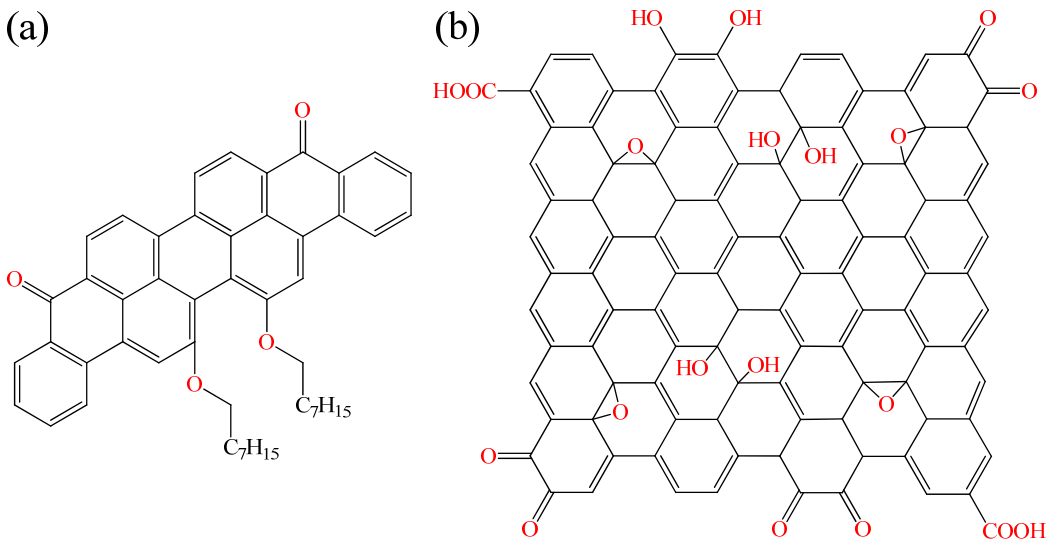

Figure 1. Molecular structures of (*a*) VO-79 and (*b*) GO employed in this work.

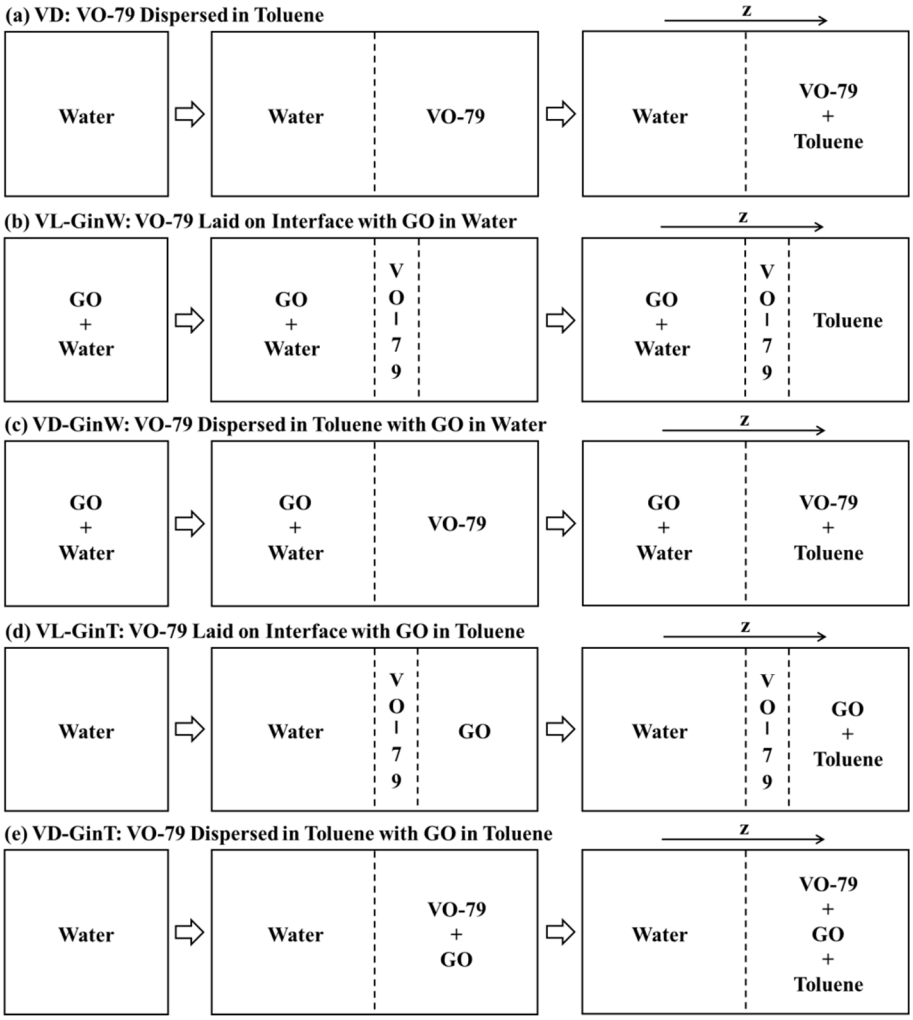

Figure 2. Schematic illustrations for constructing the initial configuration of the simulated systems.

A total of 5 systems were constructed as shown in Figure 2. The first system (named VD, "VO-79 Dispersed in Toluene"), as a control, involves a toluene/water interface with VO-79 dispersed in the toluene phase. GO is absent in this system. To build the initial configuration for this system, a simulation box of 12 × 12 × 12 nm^3 was first filled with water molecules (Figure 2a). Then, the box was expanded in the *z*-direction to a length of 24 nm, and 24 VO-79 molecules were introduced randomly into the empty space. The rest of the box was finally filled with toluene.

The next four systems were built to probe the interfacial behaviors of GO in the presence of VO-79. In general, oil-water emulsions can be categorized into O/W and W/O emulsions. If GO were used to treat O/W emulsion, it would be added to the water phase. Conversely, it would be introduced to the oil phase to treat W/O emulsion. In addition, for each type of emulsion we would like to explore two different scenarios:

one in which a protective film has not been formed by asphaltene molecules and they are still dispersed in the oil phase, and the other in which a protective film has been formed on the oil/water interface before the introduction of GO. These considerations led to the construction of the four systems described below.

Table 1. Details of the Simulated Systems

system	mimicked situation	N_{water}	$N_{toluene}$	N_{VO-79}	N_{GO}
VD	oil/water interface with asphaltene only	56582	11120	24	0
VL-GinW	GO added to O/W emulsion with asphaltene film	55368	10864	24	24
VD-GinW	GO added to O/W emulsion without asphaltene film	55182	11125	24	24
VL-GinT	GO added to W/O emulsion with asphaltene film	56706	10269	24	24
VD-GinT	GO added to W/O emulsion without asphaltene film	56582	10683	24	24

The VL-GinW system ("VO-79 Laid on interface with GO in Water") shown in Figure 2b represents GO added to O/W emulsion with a pre-formed asphaltene film on the oil/water interface. In this system, 24 GO molecules were added randomly into a simulation box of 12 × 12 × 12 nm^3, which was then filled with water. After expanding the box in *z*-direction to a length of 24 nm, 24 VO-79 molecules were laid on the toluene/water interface, followed by filling the rest of the box with toluene. The initial configuration of the VO-79 molecules here was adopted from the final configuration in the simulation of VD system (see Section S1 of the Supporting Information (SI)). The construction of VD-GinW system ("VO-79 Dispersed in toluene with GO in Water") was similar, but the 24 VO-79 molecules were introduced randomly into the toluene (Figure 2c). This system represents GO added to O/W emulsion before the formation of an asphaltene film. The next two systems represent GO added to W/O emulsion. In VL-GinT system ("VO-79 Laid on interface with GO in Toluene") shown in Figure 2d, a 12 × 12 × 12 nm^3 box was first filled with water and expanded in the *z*-direction to a length of 24 nm. Then 24 VO-79 molecules were laid on the toluene/water interface, followed by the random addition of 24 GO molecules into the empty space. The rest of the box was finally filled with toluene. Similar process was followed to build the VD-GinT system ("VO-79 Dispersed in toluene with GO in Toluene") in Figure 2e, but with VO-79 dispersed randomly in the toluene. The details of these systems are given in Table 1.

2.2 Simulation Details

The geometry of GO was first optimized at the B3LYP[35]/def2-SV(P)[36] level by using the Gaussian 09 program suite,[37] and then submitted to the Automated Topology Builder (ATB)[38] to obtain its topology compatible with the GROMOS 53A6 force field parameter set.[39] The partial atomic charges were adjusted using the CHELPG (CHarges from ELectrostatic Potentials using a Grid based method) algorithm.[40] The parameters for VO-79 and toluene were obtained with the same procedure. Water molecules were described by the well tested simple point charge (SPC) model.[41] Previous simulations using the obtained topologies have predicted properties consistent with experimental studies,[29-34,42] for example, bulk density of toluene,[42] toluene-water interfacial tension (IFT) and how it is affected by temperature, salinity and the presence of VO-79,[29-31] and the formation of GO−humic acid sandwich complex,[34] to name a few.

All simulations were carried out using the MD package GROMACS 5.0.7[43-46] with periodic boundary conditions applied in all three directions. For each system, an initial steepest descent energy minimization was performed to ensure that the maximum force was less than 1000.0 kJ/(mol·nm). This was followed by pre-equilibrations of the solvent in canonical (NVT) ensemble for 100 ps and in isothermal-isobaric (NPT) ensemble for another 100 ps, with position restraints on GO and VO-79. Then, the restraints were removed, and the system was finally sampled for 60 ns in NPT ensemble. During the production runs, temperature was kept at 300 K by v-rescaling thermostat,[47] with coupling time (τ_T) set at 0.1 ps, and pressure was controlled at 1 bar by Parrinello-Rahman barostat,[48] with coupling time (τ_P) set at 2.0 ps. LINCS algorithm was applied to constrain all bonds,[49] and the equations of motion were integrated with a time step of 2 fs. Long-range electrostatic interactions were handled by Particle Mesh Ewald (PME) method,[50,51] with a Fourier grid spacing of 0.15 nm. A twin-range cutoff scheme was used for short-range electrostatics and van der Waals (vdW) interactions with a cutoff value of 1.4 nm. Appropriate post-processing programs available in GROMACS were employed for trajectory analysis, and VMD[52] was utilized for visualization.

To calculate the toluene/water interfacial tension (IFT), each system was simulated for another 10 ns in isobaric-isothermal-isointerface area ensemble (NP_nAT) after the NPT equilibration. Here, P_n and A represent the pressure in z direction normal to the interface and the interfacial area in the xy plane, respectively. The IFT (γ) is calculated

using the following equation:[53]

$$\gamma = \frac{1}{2}\left(P_{zz} - \frac{P_{xx} + P_{yy}}{2} \right) L_z \qquad (1)$$

where P_{xx}, P_{yy}, and P_{zz} are the diagonal components of the pressure tensor, and L_z is the box length in the z direction. This approach has been employed widely to evaluate IFT from MD simulations.[29-31,54-57]

3. RESULTS AND DISCUSSION

3.1 Configuration and Energetics Analyses

Figure 3 shows the initial (left panel) and final (right panel) configurations of the 4 simulated systems: (*a*) and (*b*) for VL-GinW, (*c*) and (*d*) for VD-GinW, (*e*) and (*f*) for VL-GinT, (*g*) and (*h*) for VD-GinT. As shown in Figure 3a, initially in VL-GinW, 24 VO-79 are located at the toluene/water interface while 24 GO are randomly distributed in water. By the end of the simulation (Figure 3b), the GO molecules have moved to the interface and even entered the toluene phase. While some GO form an aggregate which is attached to the interface, most GO at the interface interact strongly with VO-79, forming a GO/VO-79 binary film which appears to have more exposure to toluene than to water. In VD-GinW (Figure 3c), VO-79 and GO molecules are initially randomly distributed in toluene and water, respectively. During the simulation, both VO-79 and GO move to the interface from the bulk, although a few VO-79 remain in bulk toluene at the final stage (Figure 3d). The VO-79 and GO arriving at the interface interact with each other and form a similar binary film. However, the formed film appears to have comparable exposure to water and toluene. In VL-GinT (Figure 3e), 24 VO-79 are placed on the interface while 24 GO are added randomly in toluene. During the simulation, most GO move from bulk toluene to the interface and interact with VO-79, while a small fraction stay in the toluene and form an aggregate (Figure 3f). A GO/VO-79 binary film is again formed on the interface. In VD-GinT (Figure 3g), both VO-79 and GO are initially distributed in toluene in a random fashion. At the end of the simulation, the majorities of GO and VO-79 have moved from toluene to the interface forming a binary film. However, some VO-79 are stabilized by GO in bulk toluene, and a GO/VO-79 co-aggregate is observed (Figure 3h). The binary films formed in both VL-GinT and VD-GinT systems appear to have more exposures to toluene than to water.

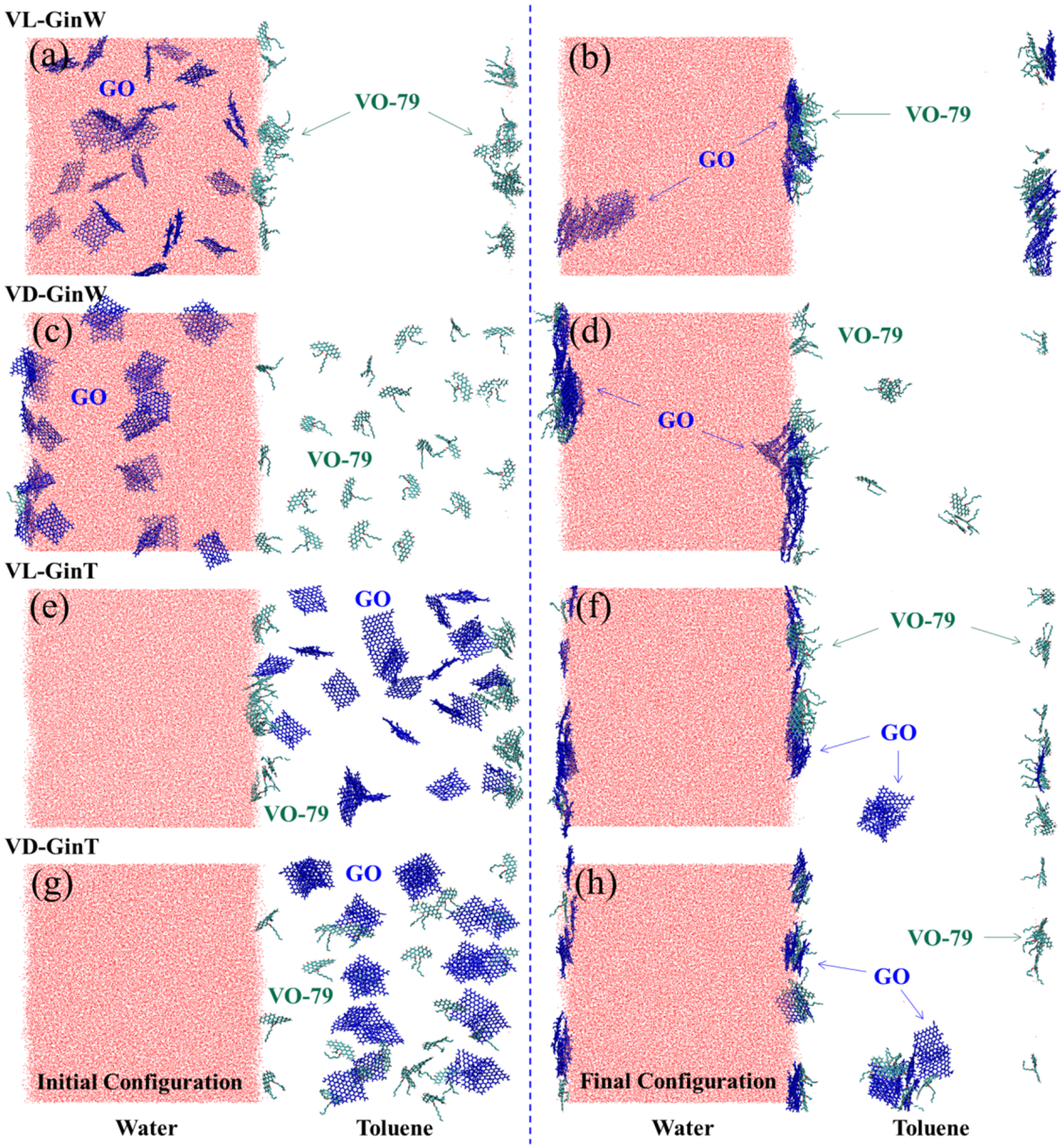

Figure 3. Initial (left panel) and final (right panel) configurations of the 4 simulated systems: (*a,b*) VL-GinW, (*c,d*) VD-GinW, (*e,f*) VL-GinT, and (*g,h*) VD-GinT. VO-79, GO and water molecules are shown in olive, blue and red, respectively. Toluene molecules are not shown for clarity.

To describe the movement of molecules in a more quantitative manner, the mass density distributions of individual components along the *z* direction (perpendicular to the interface) are plotted in Figure 4, before and after the production run. Left panel are results of t = 0 ns, which is just after the pre-equilibrations of solvent. Right panel are results obtained from average over the last 5 ns. Due to the solvent pre-equilibrations and the fact that solvent occupies majority of the volume in the simulation box, the bulk

densities of water and toluene only experience minor changes during the simulations, becoming more uniform as the solutes move to the interface. As a validation of our results, the bulk density of water from all systems is 980.3 ± 1.3 kg/m^3, and the bulk density of toluene is 861.4 ± 3.7 kg/m^3. These values agree well with the experimental values of 997.0 and 862.3 kg/m^3 at 298 K for bulk water[58] and toluene[59-61] respectively. Initially in VL-GinW (Figure 4a), VO-79 is enriched at the interface with a peak in its density profile at 12.24 nm, while the distribution of GO in water is more uniform. In the final stage of the simulation (Figure 4b), a peak in the density profile of GO appears at 12.23 nm with a height of 175.05 kg/m^3, which is an evidence for the accumulation of GO on the interface. The peak for the mass density of VO-79 has shifted to 12.32 nm with a considerable increase in height from 82.40 to 97.96 kg/m^3. In VD-GinW, GO and VO-79 both start with a random distribution, in water and toluene respectively (Figure 4c). After the simulation, GO and VO-79 gather at the interface (Figure 4d), evidenced by the appearance of two peaks: GO at 11.58 nm with a height of 235.39 kg/m^3 and VO-79 at 12.56 nm with a height of 65.24 kg/m^3. In VL-GinT, VO-79 starts with a peak in its density profile at 12.07 nm, while GO has a more or less uniform distribution in toluene (Figure 4e). After the simulation (Figure 4f), GO obtains a clear peak in its density profile at 12.09 nm with a height of 232.70 kg/m^3. The peak in the density of VO-79 has shifted to 12.23 nm with a moderate increase in peak value from 82.40 to 89.34 kg/m^3. In VD-GinT, the density profiles of GO and VO-79 both change from uniform in toluene (Figure 4g) to having a peak at the interface (Figure 4h). The peak for GO is located at 12.03 nm with a height of 189.39 kg/m^3 and the peak for VO-79 is located at 12.52 nm with a height of 71.49 kg/m^3.

At the end of the simulations, the locations of the peaks in the density profile of GO and VO-79, calculated relatively to the toluene/water interface, can be obtained. The results are shown in Section S2 of SI, along with the peak values. Except for the peak of GO in system VD-GinW, the other peaks are all located in the toluene phase. In addition, compared with the VD system where GO is absent, the peaks for the mass density of VO-79 are all located closer to the interface, suggesting that GO can create more intimate contact between water and VO-79 in toluene. Finally, it is clear from the right panel of Figure 4 that the peaks in the density profile of GO are located on the left side of the peaks for VO-79, even for the VL-GinT and VD-GinT systems where GO were initially added to toluene on the right hand side. The amphiphilic property of GO has driven them to move to the interface and even penetrate the pre-existing VO-79 film to

make contact with water.

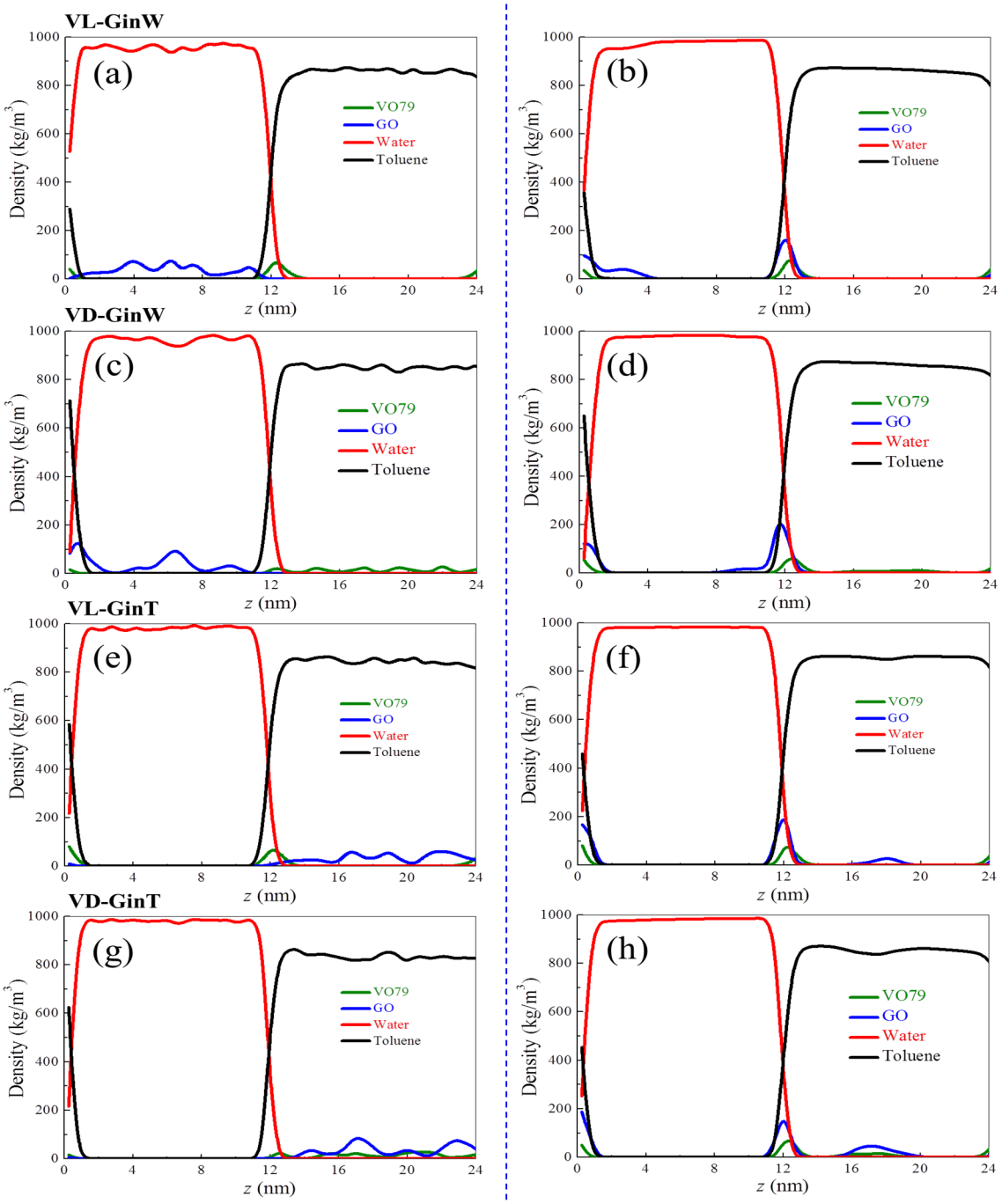

Figure 4. Initial (t = 0 ns, left panel) and final (last 5 ns, right panel) mass density distribution in z direction for VO-79 (olive), GO (blue) and solvents (water: red; toluene: black) in the 4 simulated systems: (*a,b*) VL-GinW, (*c,d*) VD-GinW, (*e,f*) VL-GinT, and (*g,h*) VD-GinT.

It is clear from the snapshots and density profiles that in all cases, there is a GO/VO-79 binary film formed at the interface. To understand the forces driving the film

formation, energetics analyses were performed and the changes in interaction energy (ΔE) between individual components are plotted in Figure 5 as functions of time. ΔE values at the end of the simulations are collected in Section S3 of SI. In all systems, ΔE between GO and VO-79 is negative and decreases with time, which indicates the attraction between the two types of molecules is beneficial for the film formation. The same is true for ΔE between GO and GO. As GO move from the bulk solvent to the interface, they change from the dispersed state to a more aggregated state (see Figure 3). The reduction in their interaction energy provides another driving force for their accumulation on the interface.

Other forces driving or resisting the binary film formation depend on where GO are placed initially. For O/W emulsion simulated by VL-GinW and VD-GinW systems (Figure 5a–5b) where GO are initially placed in the water phase, ΔE between GO and water is positive and increases with time, which implies an energy penalty as GO move from bulk water to the interface. Meanwhile, as GO form contact with toluene, their interaction energy decreases favoring the stabilization of GO on the interface. The most significant driving force for film formation in these two systems is the interaction between water molecules. The associated ΔE is negative, has very large magnitude and decreases with time. The initial dispersion of GO in water, although allowing GO and water to interact, does create a large disturbance to the hydrogen bonding network in water. As GO move to the interface, the hydrogen bonding network in bulk water is recovered, and water-water interaction energy is significantly reduced.

For W/O emulsion simulated by VL-GinT and VD-GinT systems (Figure 5c–5d) where GO are initially placed in the toluene phase, opposite to the two systems in Figure 5a–5b, ΔE between GO and water (negative and decreasing) favors film formation while ΔE between GO and toluene (positive and increasing) resists it. As GO move to the interface from bulk toluene, ΔE between toluene molecules decreases, which also facilitates the interfacial accumulation of GO. However, the magnitude of ΔE between toluene molecules is smaller than the magnitude of ΔE between GO and water, suggesting that the most significant driving force for film formation in these two systems is GO-water attraction, rather than the recovery of bulk toluene. In other words, the disturbance to bulk solvent introduced by dispersed GO molecules is less in toluene than in water, which is not surprising given the polar nature of water molecules and the resulting hydrogen bonding network formed between them. A consequence of this is that while in Figure 3b and 3d all GO molecules are attached to the interface, in Figure

3f and 3h a few GO molecules are located in bulk toluene in an aggregated form, either with VO-79 or with other GO molecules. Through aggregation, the exposure of hydrophilic groups on GO to toluene is reduced, the favorable interaction between the hydrophobic center of GO and toluene can stabilize the aggregate, and the toluene-toluene interaction is not strong enough to drive GO to the interface.

The above results have demonstrated that the formation of GO/VO-79 binary film is resisted by the interaction between GO and the solvent in which they are initially dispersed, but facilitated by the interactions between GO and VO-79, between GO themselves, between GO and the solvent they are not placed in, and between solvent molecules in which GO are initially dispersed. The other interactions shown in Figure 5 namely between VO-79 molecules, between VO-79 and solvents, and between the two solvents make minor contributions to the interfacial film formation.

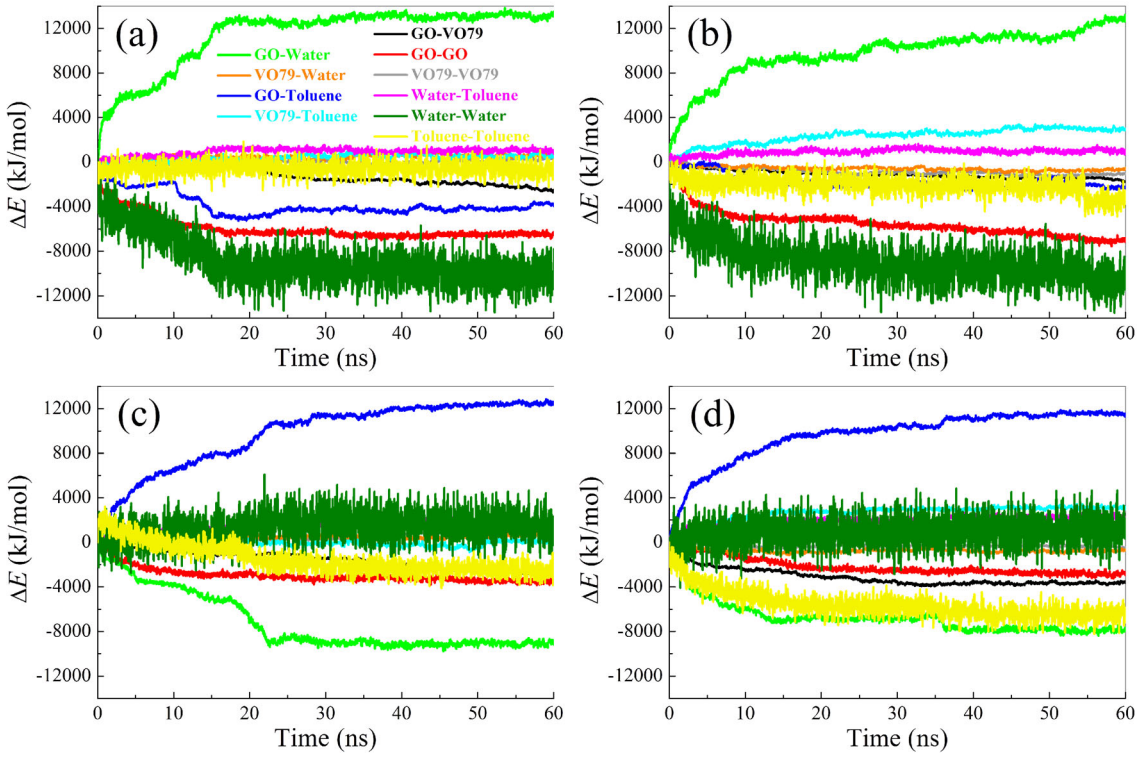

Figure 5. Time evolution of change in interaction energy (ΔE) between individual components in (a) VL-GinW, (b) VD-GinW, (c) VL-GinT, and (d) VD-GinT.

3.2 Characterization of Binary Film Formation

From the observations above, regardless of whether a VO-79 film pre-exists on the water/toluene interface, or whether GO is added to water or to toluene, a binary film is formed on the interface consisting of interconnected GO and VO-79 molecules. For a better understanding of the dynamic process of binary film formation, the numbers of

VO-79 and GO molecules adsorbed on the interface are calculated (see Section S4 of SI for details of the calculation) and plotted in Figure 6.

In VL-GinW (Figure 6a), the number of adsorbed VO-79 (black curve) fluctuates around 24 throughout the entire simulation, which is the initial number of VO-79 placed on the interface. The number of adsorbed GO (red curve) exhibits an overall increasing trend. It indicates that VO-79 are stably adsorbed on the interface with a few reversible detachments,[32,62] while GO travel continuously from the bulk water to the interface to form the binary film. In the final stage of the simulation, the number of GO adsorbed on the interface is 24, corresponding to complete adsorption of all GO molecules. During the simulation, there are three jumps in the GO curve at 10, 14, and 32 ns, respectively. These jumps can be attributed to GO adsorption in the form of an aggregate instead of monomers (Figure 3b). In VD-GinW (Figure 6b) VO-79 and GO, initially dispersed, simultaneously approach the interface, shown by the two increasing curves. The adsorption of GO is faster than VO-79, which may be caused by the stronger interfacial activity of GO. The number of adsorbed VO-79 in the final stage is noticeably less than that in VL-GinW, due to a few VO-79 that remained in bulk toluene (Figure 3d). Observation in VL-GinT (Figure 6c) is similar to that in VL-GinW, and there is a jump in the GO curve at 20 ns. However, the number of GO adsorbed at the interface is less than 24 in the final stage, which is attributed to a GO aggregate formed in the bulk toluene (Figure 3f). Behavior in VD-GinT (Figure 6d) is also similar to that in VD-GinW, but with a smaller number of adsorbed GO and VO-79 in the final stage of the simulation. This is due to a GO/VO-79 co-aggregate that was stabilized in bulk toluene (Figure 3h).

It is of interest to point out that in all systems as GO molecules are adsorbed on the interface, the fluctuations in the number of adsorbed VO-79 become smaller. It suggests that the formed binary film can stabilize the VO-79 at the interface. While the good solubility of VO-79 in toluene allows them to desorb into bulk toluene, the strong amphiphilicity of GO, as well as the attractive interactions between GO and VO-79 (see Figure 5 and Section S3 of SI), provide a stabilizing mechanism that reduces the desorption. The binary adsorption is also expected to increase the film thickness on the interface, consequently reducing the mobility of the molecules.

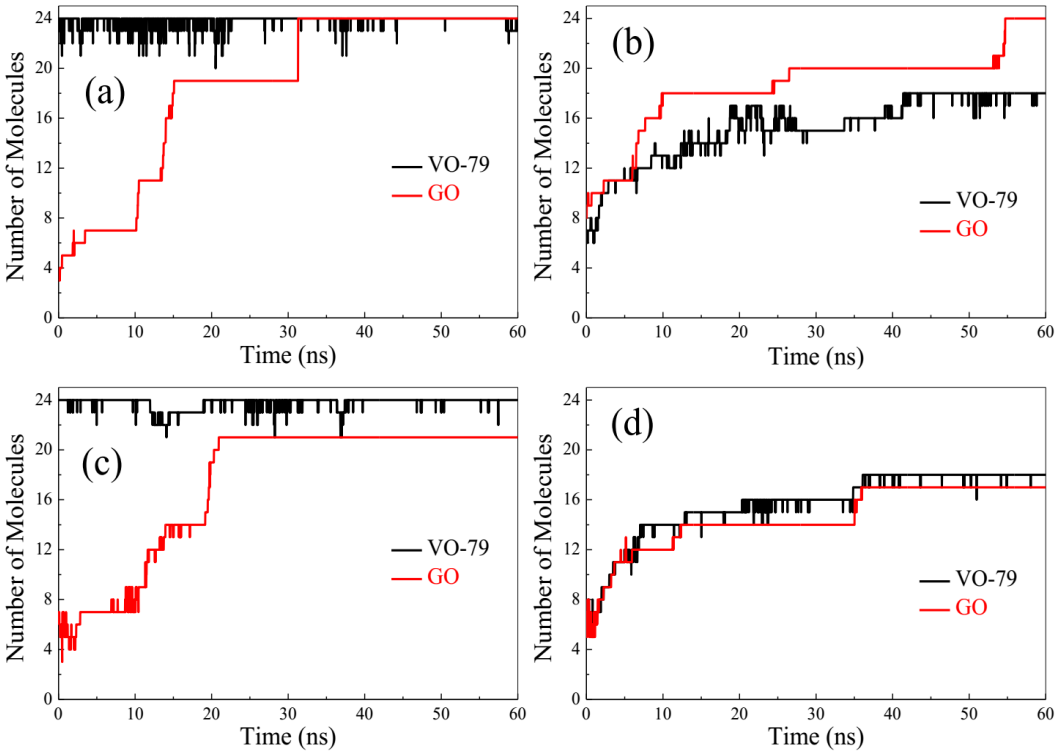

Figure 6. Number of VO-79 and GO molecules adsorbed at the interface as a function of time in (*a*) VL-GinW, (*b*) VD-GinW, (*c*) VL-GinT, and (*d*) VD-GinT.

The effective thickness of the binary film and the distribution of VO-79 and GO in the binary film, in terms of the number of molecules in water and in tolune, can be evaluated (see Section S5 of SI for details of the calculations) and the results are shown in Table 2. For the two systems with pre-adsorbed VO-79, the thickness of the binary film increases significantly after the addition of GO: from 2.99 to 4.50 nm in VL-GinW and from 2.96 to 3.45 nm in VL-GinT. These values are slightly thicker than the other two systems (VD-GinW and VD-GinT) with dispersed VO-79. From the distribution of VO-79 and GO, it can be seen that in all systems VO-79 in the binary film have significantly more exposure to toluene than to water. The results for GO, on the other hand, vary with the systems. In VL-GinT and VD-GinT mimicking W/O emulsion, the number of GO is more in toluene than in water. This is not surprising, considering that GO is initially dispersed completely in toluene. The pre-existing VO-79 layer in VL-GinT does not present a barrier for GO to approach water. In fact, compared with VD-GinT the binary film formed in VL-GinT contains more GO and the GO molecules have more exposure to water. This is because in VD-GinT a fraction of dispersed VO-79 remain in toluene and have kept some GO molecules with them via co-aggregation. There is hence a positive correlation between the total number of adsorbed VO-79 in the

film and the number of GO in the water phase. In VL-GinW and VD-GinW mimicking O/W emulsion, however, GO is initially dispersed in water. More VO-79 on the interface create a stronger pull on the GO molecules towards toluene, and hence a positive correlation exists between the total number of adsorbed VO-79 in the film and the number of GO in the toluene phase. As a result, there are more GO in toluene than in water for system VL-GinW, whereas there are more GO in water than in toluene for system VD-GinW, although the total number of GO in the film is identical in the two systems (24).

Table 2. Thickness of the Binary Film and Distribution of VO-79 and GO in the Film

system	thickness (nm)		$N_{\text{VO-79}}$		N_{GO}	
	initial film	final film	in water	in toluene	in water	in toluene
VL-GinW	2.99	4.50	1	23	10	14
VD-GinW		4.33	1	18	14	10
VL-GinT	2.96	3.45	1	23	8	13
VD-GinT		3.44	0	18	4	13

To further characterize the structure of the binary film, quantitative analysis on the orientation of VO-79 and GO molecules at the interface was conducted by calculating the angle (θ) between the positive z axis and the normal (**n**) of the VO-79 or GO plane. The calculations were performed by considering average over the last 5 ns of the simulations. Angle θ can vary from 0° to 90°. When θ is less than 20°, the plane of VO-79 or GO can be considered to be almost parallel to the interface. While θ is more than 70°, the plane is considered perpendicular to the interface. Between the two limits, the molecule is considered to be in the slant state.

The distributions of θ for the planes of VO-79 and GO are given in Figure 7. For VO-79 (Figure 7a), in VD system without GO, the angle has a wide distribution, with most molecules taking slant and parallel configurations (0°–70°) and less molecules in a perpendicular configuration (70°–90°). After the addition of GO, the number of VO-79 molecules taking a perpendicular or slant configuration reduces substantially, and more VO-79 orient themselves with their PAC plane nearly parallel to the interface (0°–20°). From Figure 7b, it is clear that the majority of GO take a parallel configuration on the interface. In so doing, the GO molecules have a large contact area with the interface and

are stably anchored. In the meantime, the VO-79 at the interface are oriented to be parallel with GO so as to enhance the interaction between them, which becomes the dominant configuration of VO-79 in the presence of GO.

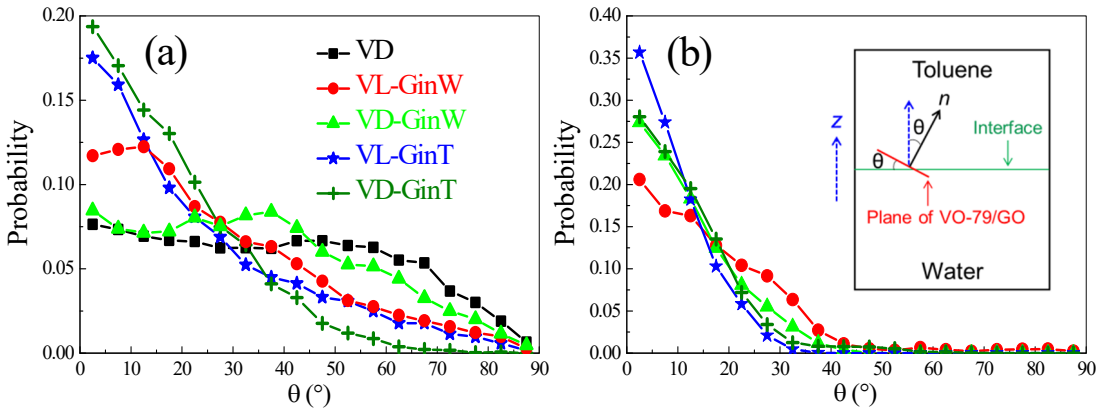

Figure 7. Distribution of orientation on the toluene/water interface for (*a*) VO-79 and (*b*) GO, averaged over the last 5 ns of the simulations. Inset: schematic depiction of the angle θ between the positive z axis and the normal (**n**) of VO-79 or GO plane.

3.3 Interfacial Tension

Surface-active chemicals from the crude oil, such as asphaltenes, can enhance emulsion stability by reducing the oil/water IFT. In turn, in most cases, demulsifiers that destabilize the emulsion cause an increase in the IFT. The toluene/water IFT of the simulated systems are shown in Table 3. As a comparison, toluene/water IFT in the absence of VO-79 and GO was calculated to be 35.41 mN/m, which is consistent with previous works.[29,63] It can be seen that in VD the VO-79 molecules on the interface cause the IFT to decrease from 35.41 to 33.52 mN/m, which promotes emulsion stability. However, the addition of GO in the next four systems all leads to an increase in the IFT, which is beneficial for emulsion destabilization. The results are consistent with previous experimental studies,[22,23,64] where adding GO can increase the oil/water IFT in the presence of asphaltenes, and the IFT monotonically increases with the GO dosage.

Table 3. Toluene/Water IFTs of the Simulated Systems

system	IFT (mN/m)
VD	33.52
VL-GinW	35.17

VD-GinW	34.43
VL-GinT	34.31
VD-GinT	34.85

440

441 ### 3.4 Implications

442 Under acid condition simulated in this work, GO molecules are found to adsorb on
443 the oil/water interface, interact with VO-79, and form a GO/VO-79 binary film. This
444 observation is consistent with previously reported results from interfacial rheology
445 tests.[23,64] In the meantime, the adsorbed GO are parallel to the interface and can induce
446 parallel alignment of VO-79, changing the original interface morphology. Based on the
447 MD results, we believe the most plausible mechanism for GO to destabilize O/W
448 emulsion is the one proposed by Fang *et al*.[23] GO can adhere to the initial asphaltene
449 film and form a new binary film around the oil droplet. When the oil droplet moves
450 close to the macroscopic oil/water interface, the binary film interacts with GO
451 assembled at the macroscopic interface, draining the oil into the bulk and realizing
452 oil-water separation. It is also possible that when two water droplets are both "coated"
453 by a binary film, the adhesion between them is enhanced by the interaction of GO
454 molecules on the outer layer. Sufficient film-film interactions could bring a large
455 number of droplets together and ultimately cause sedimentation.

456 To treat W/O emulsion, GO will be added in the oil phase. Although there have been
457 few reports on GO demulsification of W/O emulsion, we believe that the observations
458 are similar to O/W emulsion. We expect that a GO/VO-79 binary film will also form on
459 the interface, and that GO in binary film will also be located near the water phase
460 although it is initially added to the oil. Our simulations, however, suggest one possible
461 difference between W/O and O/W emulsions. In W/O emulsion, although VO-79 tend
462 to accumulate at the interface, some dispersed VO-79 could be stabilized in bulk toluene
463 by co-aggregation with GO (Figure 3h). One can therefore hypothesize that GO may
464 prevent asphaltene film formation in W/O emulsion, but not in O/W emulation.

465 Although the demulsification mechanism proposed by Liu *et al*.[18-20] was not validated
466 in this work, it may occur under neutral or alkaline condition. It is well-known that most
467 ionic surfactants are easily influenced by the solution pH. Previous studies have pointed
468 out that the effect of pH on GO demulsification is significant.[5,18] In alkaline solutions,
469 GO becomes more deprotonated, more hydrophilic, and has more tendency to remain in

the aqueous phase. As such, they may be capable of pulling asphaltenes from the interface to bulk water which subsequently aggregate. Given that previous work reported GO to be ineffective in alkaline solution,[18] this hypothesized scenario needs to be examined carefully by future simulations.

In previous experimental studies,[18-20] the dosage of GO has been shown to impact the demulsification efficiency, which increases with the GO concentration. However, when the GO concentration exceeds a threshold, its demulsification efficiency no longer increases. The threshold concentration varies with the crude sample, but is on the order of 10 to 100 mg/L. In our simulations with 24 GO molecules, the concentration of GO is calculated to be 37.3 g/L, far greater than the threshold value.[18] On the other hand, when an interfacial system is simulated in MD, it is a common practice to use a relatively high bulk concentration. This is not only due to the computational limits in MD, but also supported by the rationale that it is the surface concentration instead of bulk concentration that governs the interfacial behaviors.[29] Having a high bulk concentration in simulation essentially accelerates the diffusion process from bulk to interface that would have taken more time to occur in experiments. This approach allows us to observe the interfacial process within the timeframe permitted by MD simulations. According to our results, GO prefers to adsorb on the oil/water interface due to its amphiphilic property, and interact with VO-79 to form a GO/VO-79 binary film at the interface. We do not expect such a mechanism to change even if we lower the GO concentration in the simulations.

Finally, real crude oil is a complex mixture, and depending on its source, there can be large variations in the composition. In this work, we used a very simple representation of the oil phase and the asphaltene, which is unavoidably associated with some limitations. For example, in a real oil sample, there are some aliphatic components, such as *n*-heptane and dodecane, in which asphaltenes, as well as GO, have poor solubility. Therefore, if GO is added to treat W/O emulsion in a real oil sample, the asphaltenes and GO are expected to be more readily adsorbed at the oil/water interface forming the binary film.

4. CONCLUSIONS

A series of molecular dynamics simulations were performed to investigate the mechanism of GO to destabilize O/W and W/O emulsions in the presence of VO-79 based model asphaltenes. The snapshots and density profiles demonstrated that for both

O/W and W/O emulsions a GO/VO-79 binary film was formed, which can stabilize VO-79 at the interface. Detailed structural analysis revealed that most GO in the binary film were parallel to the interface and can induce VO-79 to be parallel with them, changing the original interface morphology. The observations from our MD simulations favor the previously proposed mechanism that GO destabilize O/W emulsions by first forming a film around the emulsion droplets and then enhancing the adhesion between droplets, or between a droplet and the macroscopic oil/water interface, through the film-film interactions. Additional IFT calculations confirmed that GO can increase the toluene/water IFT in the presence of VO-79, which is beneficial for the destabilization of emulsion. Our results provide valuable insights at atomistic level into the fundamental understanding of the mechanism of GO to destabilize O/W and W/O emulsions.

■ ASSOCIATED CONTENT

Supporting Information

The Supporting Information is available free of charge on the ACS Publications website at DOI:

Configurations in VD system, peaks in mass density profiles, change of interaction energy, calculations of the adsorbed molecules on the interface, effective thickness of the binary film and distribution of VO-79 and GO (PDF)

■ AUTHOR INFORMATION

Corresponding Authors

*E-mail: hongbo.zeng@ualberta.ca. Phone: +1-780-492-1044 (H.Z.).

*E-mail: tian.tang@ualberta.ca. Phone: +1-780-492-5467 (T.T.).

ORCID

Tu Lan: 0000-0002-9877-2636

Hongbo Zeng: 0000-0002-1432-5979

Tian Tang: 0000-0002-2387-3571

Notes

The authors declare no competing financial interest.

■ ACKNOWLEDGMENTS

We acknowledge the computing resources and technical support from Western Canada Research Grid (WestGrid). Financial support from the Natural Science and Engineering Research Council (NSERC) of Canada, and the Future Energy Systems under the Canada First Research Excellence Fund and the Canada Research Chairs Program is gratefully acknowledged.

■ REFERENCES

(1) Hummers, W. S.; Offeman, R. E. Preparation of graphitic oxide. *J. Am. Chem. Soc.* **1958,** *80*, 1339-1339.

(2) Dreyer, D. R.; Park, S.; Bielawski, C. W.; Ruoff, R. S. The chemistry of graphene oxide. *Chem. Soc. Rev.* **2010,** *39*, 228-240.

(3) Szabó, T.; Berkesi, O.; Forgó, P.; Josepovits, K.; Sanakis, Y.; Petridis, D.; Dékány, I. Evolution of surface functional groups in a series of progressively oxidized graphite oxides. *Chem. Mater.* **2006,** *18*, 2740-2749.

(4) Kim, J.; Cote, L. J.; Huang, J. Two dimensional soft material: New faces of graphene oxide. *Acc. Chem. Res.* **2012,** *45*, 1356-1364.

(5) Kim, J.; Cote, L. J.; Kim, F.; Yuan, W.; Shull, K. R.; Huang, J. Graphene oxide sheets at interfaces. *J. Am. Chem. Soc.* **2010,** *132*, 8180-8186.

(6) Kim, F.; Cote, L. J.; Huang, J. Graphene oxide: Surface activity and two-dimensional assembly. *Adv. Mater.* **2010,** *22*, 1954-1958.

(7) Cote, L. J.; Kim, J.; Tung, V. C.; Luo, J.; Kim, F.; Huang, J. Graphene oxide as surfactant sheets. *Pure Appl. Chem.* **2010,** *83*, 95-110.

(8) Tung, V. C.; Huang, J.-H.; Tevis, I.; Kim, F.; Kim, J.; Chu, C.-W.; Stupp, S. I.; Huang, J. Surfactant-free water-processable photoconductive all-carbon composite. *J. Am. Chem. Soc.* **2011,** *133*, 4940-4947.

(9) Zhang, K.; Mao, L.; Zhang, L. L.; On Chan, H. S.; Zhao, X. S.; Wu, J. Surfactant-intercalated, chemically reduced graphene oxide for high performance supercapacitor electrodes. *J. Mater. Chem.* **2011,** *21*, 7302-7307.

(10) Tung, V. C.; Kim, J.; Cote, L. J.; Huang, J. Sticky interconnect for solution-processed tandem solar cells. *J. Am. Chem. Soc.* **2011,** *133*, 9262-9265.

(11) Cao, Y.; Lai, Z.; Feng, J.; Wu, P. Graphene oxide sheets covalently functionalized with block copolymersvia click chemistry as reinforcing fillers. *J. Mater. Chem.* **2011,** *21*, 9271-9278.

(12) Male, U.; Srinivasan, P.; Singu, B. S. Incorporation of polyaniline nanofibres on graphene oxide by interfacial polymerization pathway for supercapacitor. *Int. Nano Lett.* **2015,** *5*, 231-240.

(13) Hu, R.; Zhang, R.; He, Y.; Zhao, G.; Zhu, H. Graphene oxide-in-polymer nanofiltration membranes with enhanced permeability by interfacial polymerization. *J. Membr. Sci.* **2018,** *564*, 813-819.

(14) Blake, P.; Brimicombe, P. D.; Nair, R. R.; Booth, T. J.; Jiang, D.; Schedin, F.; Ponomarenko, L. A.; Morozov, S. V.; Gleeson, H. F.; Hill, E. W., et al. Graphene-based liquid crystal device. *Nano Lett.* **2008,** *8*, 1704-1708.

(15) Xu, Z.; Gao, C. Graphene chiral liquid crystals and macroscopic assembled fibres. *Nat. Commun.* **2011,** *2*, 571.

(16) Xu, Z.; Gao, C. Aqueous liquid crystals of graphene oxide. *ACS Nano* **2011,** *5*, 2908-2915.

(17) Kim, J. E.; Han, T. H.; Lee, S. H.; Kim, J. Y.; Ahn, C. W.; Yun, J. M.; Kim, S. O. Graphene oxide liquid crystals. *Angew. Chem. Int. Ed.* **2011,** *123*, 3099-3103.

(18) Liu, J.; Li, X.; Jia, W.; Li, Z.; Zhao, Y.; Ren, S. Demulsification of crude oil-in-water emulsions driven by graphene oxide nanosheets. *Energy Fuels* **2015,** *29*, 4644-4653.

(19) Wang, H.; Liu, J.; Xu, H.; Ma, Z.; Jia, W.; Ren, S. Demulsification of heavy oil-in-water emulsions by reduced graphene oxide nanosheets. *RSC Adv.* **2016,** *6*, 106297-106307.

(20) Liu, J.; Wang, H.; Li, X.; Jia, W.; Zhao, Y.; Ren, S. Recyclable magnetic graphene oxide for rapid and efficient demulsification of crude oil-in-water emulsion. *Fuel* **2017,** *189*, 79-87.

(21) Ma, S.; Wang, Y.; Wang, X.; Li, Q.; Tong, S.; Han, X. Bifunctional demulsifier of ODTS modified magnetite/reduced graphene oxide nanocomposites for oil-water separation. *ChemistrySelect* **2016,** *1*, 4742-4746.

(22) Fang, S.; Chen, T.; Chen, B.; Xiong, Y.; Zhu, Y.; Duan, M. Graphene oxide at oil-water interfaces: Adsorption, assembly & demulsification. *Colloids Surf., A* **2016,** *511*, 47-54.
(23) Fang, S.; Chen, T.; Wang, R.; Xiong, Y.; Chen, B.; Duan, M. Assembly of graphene oxide at the crude oil/water interface: A new approach to efficient demulsification. *Energy Fuels* **2016,** *30*, 3355-3364.
(24) Xia, L.; Lu, S.; Cao, G. Stability and demulsification of emulsions stabilized by asphaltenes or resins. *J. Colloid Interface Sci.* **2004,** *271*, 504-506.
(25) Gafonova, O. V.; Yarranton, H. W. The stabilization of water-in-hydrocarbon emulsions by asphaltenes and resins. *J. Colloid Interface Sci.* **2001,** *241*, 469-478.
(26) Liu, J.; Zhao, Y.; Ren, S. Molecular dynamics simulation of self-aggregation of asphaltenes at an oil/water interface: Formation and destruction of the asphaltene protective film. *Energy Fuels* **2015,** *29*, 1233-1242.
(27) Schuler, B.; Meyer, G.; Peña, D.; Mullins, O. C.; Gross, L. Unraveling the molecular structures of asphaltenes by atomic force microscopy. *J. Am. Chem. Soc.* **2015,** *137*, 9870-9876.
(28) Kuznicki, T.; Masliyah, J. H.; Bhattacharjee, S. Aggregation and partitioning of model asphaltenes at toluene−water interfaces: Molecular dynamics simulations. *Energy Fuels* **2009,** *23*, 5027-5035.
(29) Jian, C.; Poopari, M. R.; Liu, Q.; Zerpa, N.; Zeng, H.; Tang, T. Reduction of water/oil interfacial tension by model asphaltenes: The governing role of surface concentration. *J. Phys. Chem. B* **2016,** *120*, 5646-5654.
(30) Jian, C.; Poopari, M. R.; Liu, Q.; Zerpa, N.; Zeng, H.; Tang, T. Mechanistic understanding of the effect of temperature and salinity on the water/toluene interfacial tension. *Energy Fuels* **2016,** *30*, 10228-10235.
(31) Jian, C.; Liu, Q.; Zeng, H.; Tang, T. A molecular dynamics study of the effect of asphaltenes on toluene/water interfacial tension: Surfactant or solute? *Energy Fuels* **2018,** *32*, 3225-3231.
(32) Jian, C. Y.; Liu, Q. X.; Zeng, H. B.; Tang, T. Effect of model polycyclic aromatic compounds on the coalescence of water-in-oil emulsion droplets. *J. Phys. Chem. C* **2017,** *121*, 10382-10391.
(33) Lan, T.; Liao, J.; Yang, Y.; Chai, Z.; Liu, N.; Wang, D. Competition/cooperation between humic acid and graphene oxide in uranyl adsorption implicated by molecular dynamics simulations. *Environ. Sci. Technol.* **2019,** *53*, 5102-5110.
(34) Zhou, X.; Wang, B.; Lan, T.; Chen, H.; Wang, H.; Tao, Y.; Li, Z.; Ibrahim, K.; Wang, D.; Feng, W. Chirality of graphene oxide-humic acid sandwich complex induced by a twisted, long-range-ordered nanostructure. *J. Phys. Chem. C* **2016,** *120*, 25789-25795.
(35) Becke, A. D. A new mixing of Hartree–Fock and local density-functional theories. *J. Chem. Phys.* **1993,** *98*, 1372-1377.
(36) Schäfer, A.; Horn, H.; Ahlrichs, R. Fully optimized contracted Gaussian basis sets for atoms Li to Kr. *J. Chem. Phys.* **1992,** *97*, 2571-2577.
(37) Frisch, M. J.; Trucks, G. W.; Schlegel, H. B.; Scuseria, G. E.; Robb, M. A.; Cheeseman, J. R.; Scalmani, G.; Barone, V.; Mennucci, B.; Petersson, G. A., et al. *Gaussian 09*, Gaussian, Inc.: Wallingford, CT, USA, 2009.
(38) Stroet, M.; Caron, B.; Visscher, K. M.; Geerke, D. P.; Malde, A. K.; Mark, A. E. Automated topology builder version 3.0: Prediction of solvation free enthalpies in water and hexane. *J. Chem. Theory Comput.* **2018,** *14*, 5834-5845.
(39) Oostenbrink, C.; Villa, A.; Mark, A. E.; Van Gunsteren, W. F. A biomolecular force field based on the free enthalpy of hydration and solvation: The GROMOS force-field parameter sets 53A5 and 53A6. *J. Comput. Chem.* **2004,** *25*, 1656-1676.
(40) Breneman, C. M.; Wiberg, K. B. Determining atom-centered monopoles from molecular electrostatic potentials. The need for high sampling density in formamide conformational analysis. *J. Comput. Chem.* **1990,** *11*, 361-373.
(41) Berendsen, H. J. C.; Postma, J. P. M.; van Gusteren, W. F.; Hermans, J., Interaction Models for Water in Relation to Protein Hydration. In *Intermolecular Forces*; Pullman, B., Ed; D. Reidel Publishing Company: Dordrecht, Netherlands, 1981; pp 331-342.
(42) Lan, T.; Zeng, H.; Tang, T. Understanding adsorption of violanthrone-79 as a model asphaltene compound on quartz surface using molecular dynamics simulations. *J. Phys. Chem. C* **2018,** *122*, 28787-28796.
(43) Hess, B.; Kutzner, C.; Van Der Spoel, D.; Lindahl, E. GROMACS 4: Algorithms for highly efficient, load-balanced, and scalable molecular simulation. *J. Chem. Theory Comput.* **2008,** *4*, 435-447.
(44) van der Spoel, D.; Hess, B. GROMACS—the road ahead. *Wiley Interdiscip. Rev. Comput. Mol. Sci.* **2011,** *1*, 710-715.
(45) Pronk, S.; Páll, S.; Schulz, R.; Larsson, P.; Bjelkmar, P.; Apostolov, R.; Shirts, M. R.; Smith, J. C.; Kasson, P. M.; van der Spoel, D., et al. GROMACS 4.5: A high-throughput and highly parallel open source molecular simulation toolkit. *Bioinformatics* **2013,** *29*, 845-854.

(46) Abraham, M. J.; Murtola, T.; Schulz, R.; Páll, S.; Smith, J. C.; Hess, B.; Lindahl, E. GROMACS: High performance molecular simulations through multi-level parallelism from laptops to supercomputers. *SoftwareX* **2015,** *1-2*, 19-25.
(47) Bussi, G.; Donadio, D.; Parrinello, M. Canonical sampling through velocity rescaling. *J. Chem. Phys.* **2007,** *126*, 014101.
(48) Parrinello, M.; Rahman, A. Polymorphic transitions in single crystals: A new molecular dynamics method. *J. Appl. Phys.* **1981,** *52*, 7182-7190.
(49) Hess, B. P-LINCS: A parallel linear constraint solver for molecular simulation. *J. Chem. Theory Comput.* **2008,** *4*, 116-122.
(50) Darden, T.; York, D.; Pedersen, L. Particle mesh Ewald: An N·log (N) method for Ewald sums in large systems. *J. Chem. Phys.* **1993,** *98*, 10089-10092.
(51) Essmann, U.; Perera, L.; Berkowitz, M. L.; Darden, T.; Lee, H.; Pedersen, L. G. A smooth particle mesh Ewald method. *J. Chem. Phys.* **1995,** *103*, 8577-8593.
(52) Humphrey, W.; Dalke, A.; Schulten, K. VMD: Visual molecular dynamics. *J. Mol. Graphics* **1996,** *14*, 33-38.
(53) van Buuren, A. R.; Marrink, S. J.; Berendsen, H. J. C. A molecular dynamics study of the decane/water interface. *J. Phys. Chem.* **1993,** *97*, 9206-9212.
(54) Zhang, Y.; Feller, S. E.; Brooks, B. R.; Pastor, R. W. Computer simulation of liquid/liquid interfaces. I. Theory and application to octane/water. *J. Chem. Phys.* **1995,** *103*, 10252-10266.
(55) Feller, S. E.; Venable, R. M.; Pastor, R. W. Computer simulation of a DPPC phospholipid bilayer: Structural changes as a function of molecular surface area. *Langmuir* **1997,** *13*, 6555-6561.
(56) Venable, R. M.; Brooks, B. R.; Pastor, R. W. Molecular dynamics simulations of gel ($L_{\beta I}$) phase lipid bilayers in constant pressure and constant surface area ensembles. *J. Chem. Phys.* **2000,** *112*, 4822-4832.
(57) Kunieda, M.; Nakaoka, K.; Liang, Y.; Miranda, C. R.; Ueda, A.; Takahashi, S.; Okabe, H.; Matsuoka, T. Self-accumulation of aromatics at the oil−water interface through weak hydrogen bonding. *J. Am. Chem. Soc.* **2010,** *132*, 18281-18286.
(58) O'Neil, M. J. *The Merck Index: An Encyclopedia of Chemicals, Drugs, and Biologicals*; RSC Publishing: Cambridge, UK, 2013.
(59) Assael, M.; Avelino, H.; Dalaouti, N.; Fareleira, J.; Harris, K. Reference correlation for the viscosity of liquid toluene from 213 to 373 K at pressures to 250 MPa. *Int. J. Thermophys.* **2001,** *22*, 789-799.
(60) Muringer, M.; Trappeniers, N.; Biswas, S. The effect of pressure on the sound velocity and density of toluene and *n*-heptane up to 2600 bar. *Phys. Chem. Liq.* **1985,** *14*, 273-296.
(61) Kashiwagi, H.; Hashimoto, T.; Tanaka, Y.; Kubota, H.; Makita, T. Thermal conductivity and density of toluene in the temperature range 273–373 K at pressures up to 250 MPa. *Int. J. Thermophys.* **1982,** *3*, 201-215.
(62) Jian, C.; Zeng, H.; Liu, Q.; Tang, T. Probing the adsorption of polycyclic aromatic compounds onto water droplets using molecular dynamics simulations. *J. Phys. Chem. C* **2016,** *120*, 14170-14179.
(63) Donahue, D. J.; Bartell, F. E. The boundary tension at water-organic liquid interfaces. *J. Phys. Chem.* **1952,** *56*, 480-484.
(64) Sun, Z.; Feng, T.; Russell, T. P. Assembly of graphene oxide at water/oil interfaces: Tessellated nanotiles. *Langmuir* **2013,** *29*, 13407-13413.

697 **TOC Graphic:**

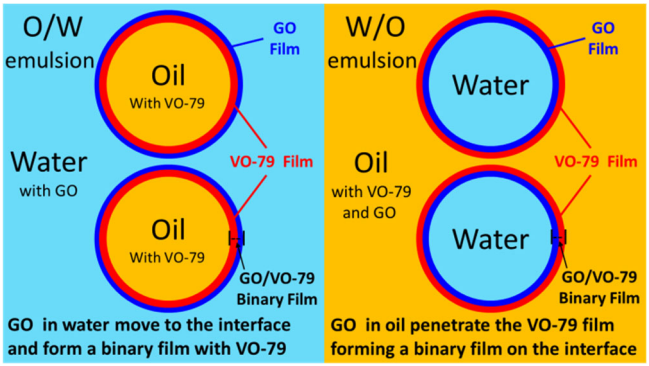

698